Journal of Organometallic Chemistry 824 (2016) 42–47

Contents lists available at ScienceDirect

Journal of Organometallic Chemistry

journal homepage: www.elsevier.com/locate/jorganchem

Mono- and tetranuclear cyclopalladated complexes with *N*′-(9-anthracenylidene)benzothiohydrazide: Syntheses, structures and catalytic applications

G. Narendra Babu, Samudranil Pal*

School of Chemistry, University of Hyderabad, Hyderabad, 500 046, India

ARTICLE INFO

Article history:
Received 11 August 2016
Received in revised form
28 September 2016
Accepted 30 September 2016
Available online 1 October 2016

Keywords:
Cyclopalladates
N′-(9-anthracenylidene)benzothiohydrazide
Crystal structures
Spectroscopic properties
C(sp)–C(sp) coupling

ABSTRACT

Reaction of $PdCl_2$, LiCl, *N*′-(9-anthracenylidene)benzothiohydrazide (H_2L, 2 Hs represent the thioamide NH proton and the 9-anthracenylidene *peri* proton) and $NaOAc\cdot 3H_2O$ in 1:2:1:1 mole ratio in methanol produced $[Pd_4(L)_4]$ (**1**) in 75% yield. Treatment of **1** with PPh_3 (1:4.5 mole ratio) in acetone provided $[Pd(L)(PPh_3)]$ (**2**) in 72% yield. The molecular formulas of the diamagnetic and non-electrolytic **1** and **2** were established by elemental analyses. Molecular structures of **1** and **2** were determined by single crystal X-ray diffraction studies. In the tetranuclear **1**, the palladium(II) centers are in distorted square-planar CNS_2 coordination environments created by four $(L)^{2-}$, each of which acts as 5,6-membered fused chelate rings forming thioamidate-S, azomethine-N and 9-anthracenylidene *peri*-C donor to one metal center and uses the thioamidate-S atom to bridge a second metal center. In the mononuclear **2**, $(L)^{2-}$ and PPh_3 assemble a distorted square-planar CNSP coordination environment around the palladium(II) center. Spectroscopic (IR, NMR and UV-Vis) measurements were also used to characterize **1** and **2**. The catalytic properties of both complexes in the oxidative phenylacetylene homocoupling reaction were examined.

1. Introduction

Since the discovery of the first cyclometallated complex [1], such species remain of considerable contemporary interest due to their potential applications in a variety of research areas such as organic synthesis, materials science and biological and medicinal chemistry [2–9]. As a consequence, there are continuous efforts towards the synthesis of new cyclometallated complexes. Over the past several years, we have been working on cyclometallates of platinum metal ions with aroylhydrazones and thiosemicarbazones of various mono- and polycyclic aromatic aldehydes [10–16]. It has been found that five-membered ring forming azomethine-N and amidate-O or thioamidate-S chelation by aroylhydrazonates or thiosemicarbazonates facilitates cyclometallation via not only $C(sp^2)$–H [10–15] but also $C(sp^3)$–H [16] activation. The aroylhydrazonates or the thiosemicarbazonates act as pincer-like CNO- or CNS-donor in the final cyclometallated complexes formed. In the present work, to examine whether *N*′-(9-anthracenylidene)benzothiohydrazide (H_2L) behaves in the same way or not we have explored its chemistry with palladium(II) and isolated a mononuclear cyclopalladate and a teranuclear cyclopalladate (Scheme 1). Herein we report the syntheses, crystal structures and spectroscopic properties of these two complexes and their catalytic applications in oxidative homocoupling of phenylacetylene.

2. Experimental

2.1. Materials

The Schiff base *N*′-(9-anthracenylidene)benzothiohydrazide (H_2L) was synthesized from equimolar amounts of 9-anthraldehyde and thiobenzhydrazide by following a slightly modified (using methanol instead of ethanol as solvent) reported procedure [17]. All other chemicals used in this work were of reagent grade available commercially and were used as received without any further purification. Standard methods [18] were employed for purification of the solvents used.

* Corresponding author.
E-mail address: spal@uohyd.ac.in (S. Pal).

http://dx.doi.org/10.1016/j.jorganchem.2016.09.032
0022-328X/

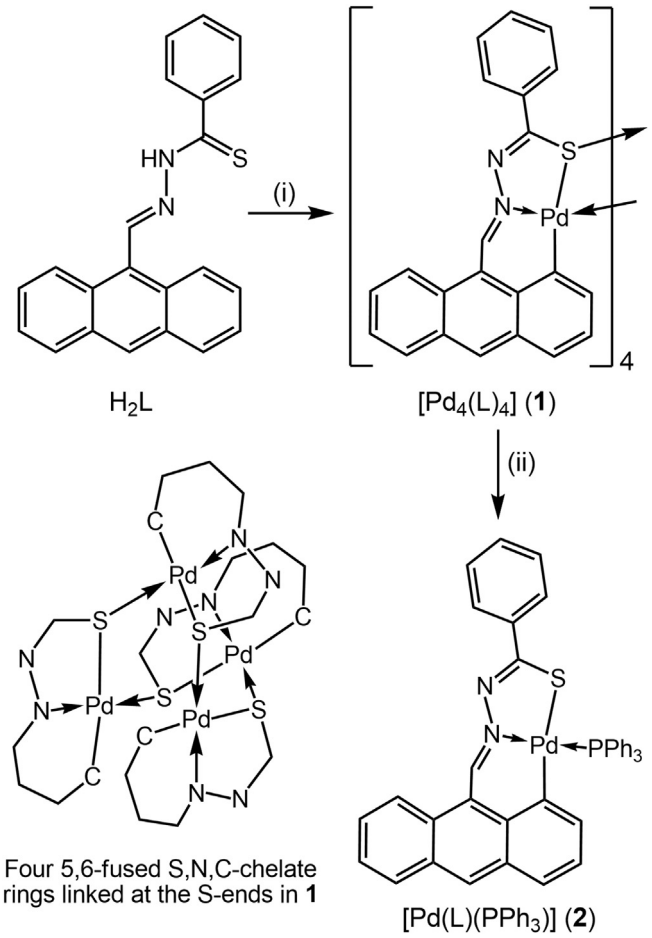

Scheme 1. (i) $PdCl_2$, LiCl and $NaOAc{\cdot}3H_2O$ (1:2:1 mole ratio) in methanol at 298 K. (ii) PPh_3 (4.5 molar equivalents) in acetone at 298 K.

2.2. Physical measurements

Elemental (CHN) analysis data were obtained using a Thermo Finnigan Flash EA1112 series elemental analyzer. A Shimadzu LCMS 2010 liquid chromatograph mass spectrometer was used to verify the purity of H_2L. Magnetic susceptibility measurements at room temperature were performed with a Sherwood scientific balance. A Thermo Scientific Nicolet 380 FT-IR spectrophotometer was employed to collect the infrared spectra. A Digisun DI-909 conductivity meter was used for solution electrical conductivity measurements. Electronic spectra were recorded on a Shimadzu UV3600 UV-Vis-NIR spectrophotometer. The ^1H (400 MHz, $SiMe_4$ as an internal standard) and $^{31}P\{^1H\}$ (160 MHz, 85% H_3PO_4 as an external standard) NMR spectra were recorded with the help of a Bruker NMR spectrometer. A Shimadzu GCMS-QP2010 gas chromatograph mass spectrometer was used for GC-MS analysis.

2.3. Synthesis of $[Pd_4(L)_4]$ (**1**)

A mixture of $PdCl_2$ (90 mg, 0.5 mmol), LiCl (43 mg, 1 mmol), H_2L (171 mg, 0.5 mmol) and $NaOAc{\cdot}3H_2O$ (69 mg, 0.5 mmol) in 40 ml methanol was stirred at room temperature (298 K) for 2 days. The brick red solid separated was collected by filtration, dissolved in minimum amount of dichloromethane and added to a silica gel column (packed with a *n*-hexane slurry of silica gel). Elution with *n*-hexane–ethylacetate (3:7) mixture initially provided a light yellow band which was discarded. The following brick red band containing **1** was collected and evaporated to dryness. Yield: 170 mg (75%). Anal. Calcd for $C_{88}H_{56}N_8S_4Pd_4$: C, 59.40; H, 3.17; N, 6.30. Found: C, 59.27; H, 3.23; N, 6.38. Selected IR data: ν (cm^{-1}) = 1594 & 1581 (N=C–C=N), 945 (C–S). UV-Vis in CH_2Cl_2: λ_{max} (nm) (10^4 x ε (M^{-1} cm^{-1})) = 562 (0.93), 525 (1.10), 490 (1.04), 392 (1.33), 376 (1.19). ^1H NMR in $CDCl_3$: δ (ppm) (J (Hz)) = 9.37 (s, 1H), 8.87 (s, 1H), 8.47 (7) (d, 2H), 7.96 (9) (d, 1H), 7.77 (s, 1H), 7.75 (2) (d, 1H), 7.63 (s, 1H), 7.43 (4) (d, 2H), 7.21–7.13 (m, 3H), 6.57 (8) (t, 1H).

2.4. Synthesis of $[Pd(L)(PPh_3)]$ (**2**)

To a suspension of $[Pd_4(L)_4]$ (**1**) (135 mg, 0.076 mmol) in acetone (20 ml) solid PPh_3 (90 mg, 0.34 mmol) was added. The resulting mixture was stirred at room temperature (298 K) for one day. The orange red solid obtained was filtered off, dissolved in minimum amount of dichloromethane and transferred to a silica gel column (packed with a silica gel slurry in *n*-hexane). Elution with *n*-hexane–ethylacetate (9:1) gave an orange red band containing **2**. This band was collected and evaporated to dryness. Yield: 155 mg (72%). Anal. Calcd for $C_{40}H_{29}N_2SPPd$: C, 67.94; H, 4.13; N, 3.96. Found: C, 67.85; H, 4.18; N, 4.07. Selected IR data: ν (cm^{-1}) = 1596 & 1581 (N=C–C=N), 941 (C–S), 742, 691 and 536 (PPh_3). UV-Vis in CH_2Cl_2: λ_{max} (nm) (10^4 x ε (M^{-1} cm^{-1}) = 550^{sh} (0.73), 511 (1.27), 485^{sh} (1.14), 390 (0.65), 370 (0.56). ^1H NMR in $CDCl_3$: δ (ppm) (J (Hz)) = 9.99 (10) (d, 1H), 8.68 (9) (d, 1H), 8.66 (s, 1H), 8.17 (8) (d, 2H), 8.11 (8) (d, 1H), 7.71–7.65 (m, 8H), 7.60–7.56 (m, 2H), 7.47–7.42 (m, 3H), 7.39–7.35 (m, 9H), 6.72 (8) (t, 1H). $^{31}P\{^1H\}$ NMR in $CDCl_3$: δ (ppm) = 36.26.

2.5. X-ray crystallography

Single crystals of $[Pd_4(L)_4]$ (**1**) were grown by slow evaporation of its solution in chloroform-acetonitrile (1:1), while slow evaporation of an acetonitrile solution of $[Pd(L)(PPh_3)]$ (**2**) provided its single crystals. Both **1** and **2** crystallized as solvates – **1**·$CHCl_3$ and **2**·CH_3CN, respectively. Unit cell determination and intensity data collection for both crystals were performed at 298 K on an Oxford Diffraction Xcalibur Gemini single crystal X-ray diffractometer using graphite monochromated Mo $K\alpha$ radiation (λ = 0.71073 Å). The CrysAlisPro software [19] was used for data collection, reduction and absorption correction. The structures of both **1**·$CHCl_3$ and **2**·CH_3CN were solved by direct methods and refined on F^2 by full-matrix least-squares procedures. In the case of **1**, the phenyl rings of the thiobenzoyl moieties of two $(L)^{2-}$ were refined with geometric restraints. A few additional significant residual electron density peaks (38 e^- per unit cell in a total potential solvent-accessible void volume of 1940.2 $Å^3$) which could not be refined as disordered solvent molecules were dealt with SQUEEZE procedure [20] as implemented in the Platon package [21]. In both structures, all non-hydrogen atoms were refined anisotropically. The hydrogen atoms were placed in geometrically idealized positions and refined by using a riding model. SHELX-97 programs [22] used for structure solution and refinement were accessed through the WinGX package [23]. Thermal ellipsoid plots were prepared using the Mercury [24] package. Selected crystallographic data for both structures are summarized in Table 1.

2.6. Procedure for the homocoupling of phenyl acetylene

To a mixture of phenylacetylene (1 mmol), K_3PO_4 (1.5 mmol) and cocatalyst CuI (0.5 mol%) in acetonitrile (1 ml) a dimethylformamide solution (0.1 ml) of catalyst (**1** or **2**) (0.1 mol%) was added. The reaction mixture was stirred at 60 °C for the required time and then cooled to room temperature. It was transferred to a separating funnel containing water (20 ml) and extracted with

Table 1
Selected crystal data and structure refinement summary.

Complex	$1\cdot CHCl_3$	$2\cdot CH_3CN$
Chemical formula	$C_{89}H_{57}Cl_3N_8S_4Pd_4$	$C_{42}H_{32}N_3PSPd$
Formula weight	1898.62	748.14
Crystal system	Tetragonal	Monoclinic
Space group	$I4_1/a$	$P2_1/n$
a (Å)	44.5189(10)	12.4885(18)
b (Å)	44.5189(10)	12.9202(19)
c (Å)	15.3784(5)	21.517(3)
α (°)	90	90
β (°)	90	105.596(9)
γ (°)	90	90
V (Å^3), Z	30478.9(14), 16	3344.0(8), 4
ρ_{calcd} (g cm^{-3})	1.655	1.486
μ (mm^{-1})	1.198	0.701
Refl. collected	29976	12756
Refl. unique	13418	5880
Refl. [$I \geq 2\sigma(I)$]	8547	4324
Parameters	973	434
$R1$, w$R2$ [$I \geq 2\sigma(I)$]	0.0688, 0.1369	0.0417, 0.0841
$R1$, w$R2$ [all data]	0.1143, 0.1531	0.0656, 0.0944
GOF on F^2	1.062	1.026
Max./Min. $\Delta\rho$ (e Å^{-3})	0.769/−0.509	0.502/−0.439

ethylacetate (20 ml). The ethylacetate extract was washed with water (2 × 10 ml), dried over anhydrous Na_2SO_4 and finally subjected to GC-MS analysis for confirmation of the product and determination of its yield.

3. Results and discussion

3.1. Synthesis and characterization

The Schiff base *N′*-(9-anthracenylidene)benzothiohydrazide (H_2L) was synthesized in *ca.* 90% yield by the condensation reaction of equimolar amounts of benzothiohydrazide and 9-anthraldehyde in methanol in presence of a few drops of acetic acid [17]. The identity and purity of H_2L were confirmed by elemental analysis, LC-MS and spectroscopic (IR and ^{1}H NMR) measurements. Reaction of Li_2PdCl_4 (prepared in situ), H_2L and $NaOAc\cdot 3H_2O$ in 1:1:1 mole ratio in methanol afforded a tetranuclear palladium(II) complex of molecular formula $[Pd_4(L)_4]$ (**1**) in 75% yield. Treatment of **1** with *ca.* 4.5 molar equivalent of PPh_3 in acetone produced the mononuclear palladium(II) complex having the molecular formula $[Pd(L)(PPh_3)]$ (**2**) in 72% yield (Scheme 1). Elemental analysis data of **1** and **2** are in good agreement with their corresponding molecular formulas. Both complexes are diamagnetic. Thus the palladium centers in them are bivalent and they are in square-planar coordination environment. The tetranuclear complex (**1**) is brick-red, while the mononuclear complex (**2**) is orange-red in color. They are highly soluble in dichloromethane, chloroform, dimethylsulfoxide and dimethylformamide; sparingly soluble in acetonitrile, methanol and toluene and insoluble in *n*-hexane. The electrically non-conducting behavior of both **1** and **2** in solution is consistent with them being neutral molecular species.

3.2. X-ray molecular structures

The molecular structures of **1** and **2** are illustrated in Figs. 1 and 2, respectively. The bond lengths and angles related to the metal centers are listed in Tables 2 and 3. In both complexes, the metal centers are in distorted square-planar coordination environments. In the tetranuclear **1**, each $(L)^{2-}$ binds one palladium atom through the thioamidate-S, the azomethine-N and the 9-anthracenylidene *peri*-C atoms to form a 5,6-membered fused chelate rings motif and uses the thioamidate-S again to coordinate a second palladium atom (Scheme 1 and Fig. 1). As a result, all four palladium centers are in planar CNS_2 (rms deviations from the mean plane are in the range 0.03–0.06 Å) environments. The $\{Pd_4(\mu\text{-}S)_4\}$ core has a cradle-like structure (Fig. 1, inset). The metal···metal distances in the four Pd–S–Pd fragments are in the range 3.8859(9)–4.0912(8) Å, while those in the two pairs of unbridged palladium centers are comparatively much shorter (Pd(1)···Pd(2), 3.3636(9) Å and Pd(3)···Pd(4), 3.2592(9) Å). It may be noted that a tetrapalladium(II) complex with a CNS-donor thiosemicarbazonate ligand [25]

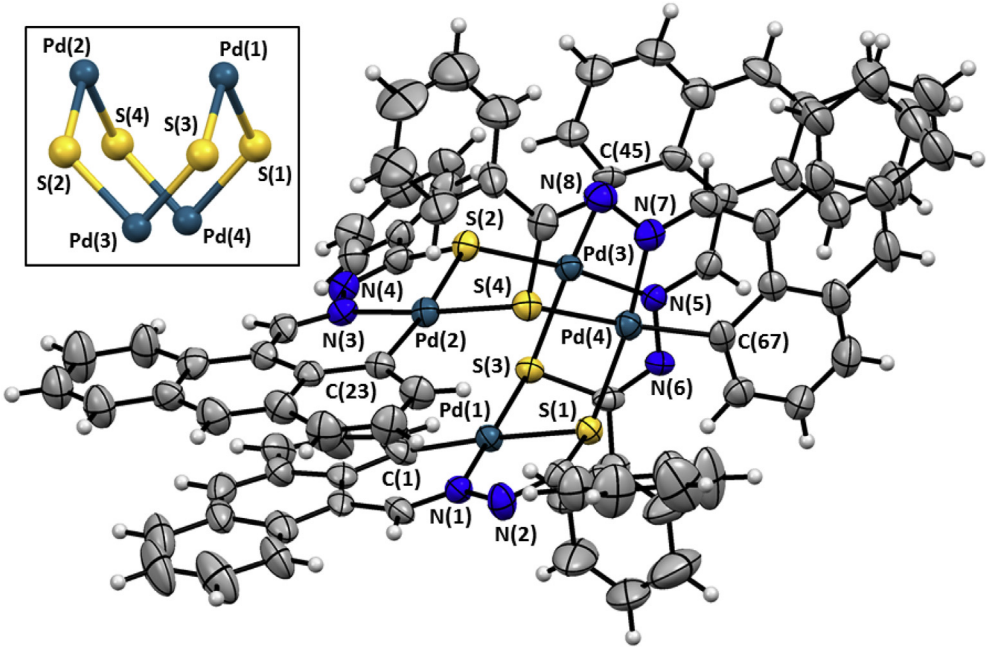

Fig. 1. ORTEP representation of $[Pd_4(L)_4]$ (**1**) and the cradle-like $\{Pd_4(\mu\text{-}S)_4\}$ core (inset). All non-hydrogen atoms are shown at their 40% probability thermal ellipsoids. All non-carbon atoms and only the metallated carbons are labeled for clarity.

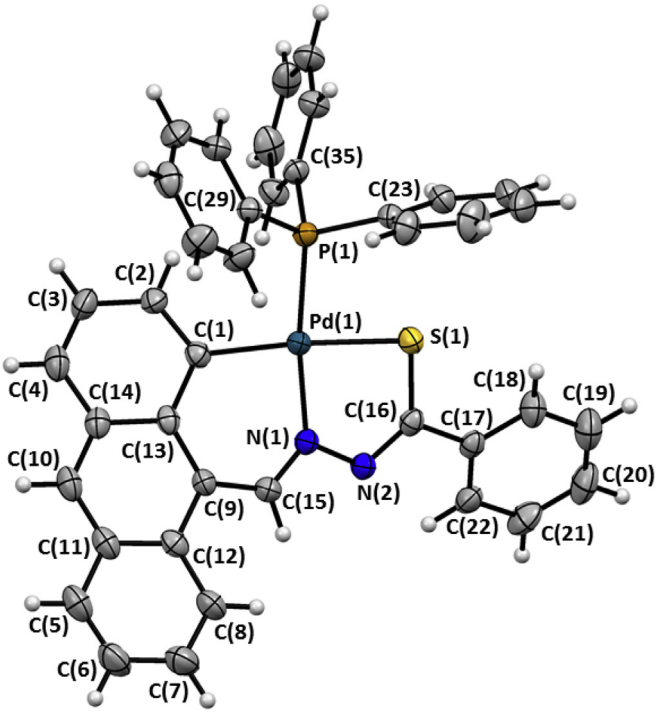

Fig. 2. ORTEP representation of [Pd(L)(PPh_3)] (**2**) with the atom labeling scheme. The thermal ellipsoids of all non-hydrogen atoms are drawn at the 40% probability level.

Table 2
Selected bond lengths (Å) and angles (°) for $[Pd_4(L)_4]\cdot CHCl_3$ (**1**·$CHCl_3$).

Pd(1)–C(1)	2.026(7)	Pd(3)–C(45)	2.044(7)
Pd(1)–N(1)	1.995(6)	Pd(3)–N(5)	1.994(6)
Pd(1)–S(1)	2.3376(19)	Pd(3)–S(3)	2.319(2)
Pd(1)–S(3)	2.312(2)	Pd(3)–S(2)	2.345(2)
Pd(2)–C(23)	2.028(8)	Pd(4)–C(67)	2.035(8)
Pd(2)–N(3)	2.001(6)	Pd(4)–N(7)	1.987(7)
Pd(2)–S(2)	2.329(2)	Pd(4)–S(4)	2.331(2)
Pd(2)–S(4)	2.338(2)	Pd(4)–S(1)	2.357(2)
C(1)–Pd(1)–N(1)	91.7(3)	C(45)–Pd(3)–N(5)	91.6(3)
C(1)–Pd(1)–S(1)	175.4(2)	C(45)–Pd(3)–S(3)	174.2(2)
C(1)–Pd(1)–S(3)	93.1(2)	C(45)–Pd(3)–S(2)	94.6(2)
N(1)–Pd(1)–S(1)	84.16(17)	N(5)–Pd(3)–S(3)	83.73(19)
N(1)–Pd(1)–S(3)	173.33(19)	N(5)–Pd(3)–S(2)	173.37(19)
S(3)–Pd(1)–S(1)	91.18(7)	S(3)–Pd(3)–S(2)	90.25(7)
C(23)–Pd(2)–N(3)	91.7(3)	C(67)–Pd(4)–N(7)	91.4(3)
C(23)–Pd(2)–S(2)	173.5(2)	C(67)–Pd(4)–S(4)	173.0(3)
C(23)–Pd(2)–S(4)	94.2(2)	C(67)–Pd(4)–S(1)	96.0(3)
N(3)–Pd(2)–S(2)	82.95(19)	N(7)–Pd(4)–S(4)	82.9(2)
N(3)–Pd(2)–S(4)	174.1(2)	N(7)–Pd(4)–S(1)	172.6(2)
S(2)–Pd(2)–S(4)	91.14(7)	S(4)–Pd(4)–S(1)	89.70(7)

also has the molecular structure very similar to that of **1**. In the mononuclear **2**, $(L)^{2-}$ acts as CNS-donor and the P-atom of PPh_3 occupies the fourth coordination site (Fig. 2). The CNSP coordination environment around the metal center in **2** is not so planar (rms deviation from the mean plane is 0.13 Å) as that of the CNS_2 environment in **1**. This slight non-planarity is perhaps due to the steric effect of the PPh_3. Overall, the metal centered bond lengths in **1** and **2** are comparable with those observed for palladium(II) complexes having similar coordinating atoms [25–28].

Table 3
Selected bond lengths (Å) and angles (°) for [Pd(L)(PPh_3)]·CH_3CN (**2**·CH_3CN).

Pd(1)–C(1)	2.021(3)	Pd(1)–S(1)	2.3126(9)
Pd(1)–N(1)	2.005(3)	Pd(1)–P(1)	2.2659(10)
C(1)–Pd(1)–N(1)	90.43(12)	N(1)–Pd(1)–S(1)	82.61(8)
C(1)–Pd(1)–S(1)	169.77(11)	N(1)–Pd(1)–P(1)	170.91(9)
C(1)–Pd(1)–P(1)	96.37(10)	S(1)–Pd(1)–P(1)	91.39(3)

3.3. Spectroscopic properties

Infrared spectra of all the compounds were recorded in the range 4000–400 cm^{-1} using KBr pellets. Each compound displayed a large number of bands of various intensities. Except for the following few selected bands no attempt was made to assign the other bands. The spectrum of the free Schiff base H_2L showed the thioamide N–H and C=S stretches as a broad strong band at 3183 cm^{-1} and as a sharp strong band at 954 cm^{-1}, respectively [17,26,29]. The disappearance of the N–H stretching band and appearance of the C=S stretching band at lower frequency (*ca.* 943 cm^{-1}) with less intensity in the spectra of **1** and **2** indicate the thioamidate-S coordination to the metal center in both complexes. A medium intensity band observed for H_2L at 1594 cm^{-1} is attributed to the C=N stretching. On the other hand, both **1** and **2** displayed two closely spaced medium to strong bands at *ca.* 1595 and 1581 cm^{-1}. These bands are most likely associated with the one end coordinated conjugated –N=C–C=N– moiety of the ligand $(L)^{2-}$ (Scheme 1). The presence of the coordinated PPh_3 in the mononuclear **2** is indicated by the characteristic three strong bands at 742, 691 and 536 cm^{-1} [15,16,27].

Electronic absorption spectra of **1** and **2** were recorded in dichloromethane. Both complexes exhibited a strong band in the visible region (*ca.* 518 nm) flanked on both sides by two shoulders and two more strong bands in the ultraviolet region (*ca.* 391 and 373 nm) (Fig. 3). It may be noted that the spectrum of the free Schiff base (H_2L) displayed a shoulder at 435 nm and a group of four rather closely spaced strong bands in the range 395–335 nm followed by a very strong absorption at 257 nm [17]. This spectral profile of H_2L is very similar to that of anthracene containing Schiff bases and free anthracene [11,30,31]. Except for the red shift, the visible region absorption profiles of **1** and **2** are somewhat similar to the spectral profile observed for H_2L [17]. Thus it is very likely that the structured visible region absorption as well as the couple of higher energy absorptions displayed by the complexes **1** and **2** are largely due to ligand centered transitions only [11,13–15]. Further,

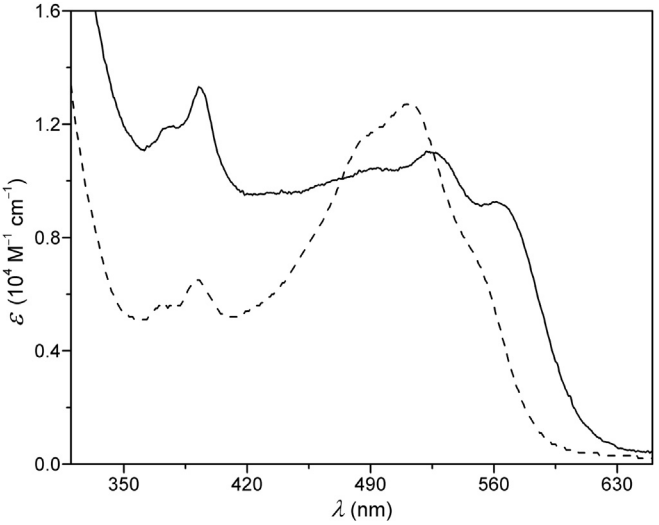

Fig. 3. Electronic spectra of $[Pd_4(L)_4]$ (**1**) (——) and [Pd(L)(PPh_3)] (**2**) (– – –) in dichloromethane.

metallation of the aromatic ring is also known to cause red shift of absorption bands related to $\pi-\pi^*$ transitions [11,13–15,28,32].

The ^{1}H NMR spectra of **1** and **2** were recorded in $CDCl_3$. The spectrum of **1** indicated that its four {Pd(L)} units are equivalent to each other. None of the two complexes displayed the singlet resonance of the thioamide N–H proton observed for the free H_2L at δ 13.45 ppm [17]. Thus in each of **1** and **2** the thioamide fragment is deprotonated. The azomethine proton of H_2L resonates as a singlet at δ 9.96 ppm. A singlet observed at δ 9.37 ppm for **1** is attributed to the proton of the azomethine group that is coordinated to the metal via the N-atom. In contrast, the azomethine proton in **2** appeared as a doublet ($J = 10$ Hz) at δ 9.99 ppm due to coupling with the PPh_3 P-atom at the coordination site *trans* to the azomethine-N. The chemical shift ranges and the intensities of the signals corresponding to the aromatic protons of both **1** (δ 8.87–6.57 ppm) and **2** (δ 8.68–6.72 ppm) are unexceptional and as expected. The $^{31}P\{^1H\}$ NMR spectrum of **2** exhibited a singlet at δ 36.26 ppm, corresponding to the PPh_3 ligand present in it.

3.4. Catalytic activities

Conjugated 1,3-diynes derived via cross coupling of sp-hybridized carbons have been found to be very useful and effective synthons for a variety of biologically active natural products, pharmaceuticals and also functional materials [33–38]. The first oxidative homocoupling reaction of the terminal alkyne phenylacetylene using CuCl in ammoniacal ethanol medium in presence of air was reported way back in 1869 by Glaser [39,40]. Since then the original procedure has been modified every now and then by varying the catalyst composition, base, oxidant and solvent to broaden its applications. Among various catalysts employed so far, quite a few were copper/palladium based [33–38]. Majority of the palladium cocatalysts used were either palladium(II) salts or palladium(0/II) coordination complexes. To the best of our knowledge there are only two reports on the use of cyclopalladated complexes as catalysts [41,42]. Hence, we examined the catalytic properties of the present cyclometallated complexes **1** and **2** in the homocoupling of phenylacetylene. Optimization of the reaction conditions was performed by varying the base and its amount, solvent (1 ml) and temperature using 1 mmol of the substrate phenylacetylene and **2** (0.1 mol% in 0.1 ml dimethylformamide) with CuI (0.5 mol%) as the catalyst system in presence of air (Table 4). In each attempt, the reaction was considered complete when there was no change of the substrate concentration. The best condition was found to be the use of K_3PO_4 (1.5 mmol) as the base and acetonitrile as the solvent at a temperature of 60 °C (entry 12). Under this condition in 4 h the reaction was complete and 93% yield was obtained. In the control experiments, 48% yield was obtained without **2** (entry 23) and 29% yield was obtained in the absence of CuI (entry 24). In the previously reported first instance of cyclopalladate catalyzed homocoupling of terminal alkynes, a dinuclear *ortho*-metallated complex $[Pd_2(\mu\text{-}Cl)_2(L')_2]$ (0.05 mol%) (HL' = 4,4'-dichlorobenzophenone oxime) and CuI (5 mol%) were used as the catalyst mixture [41]. The reactions performed in N-methylpyrrolidinone solvent in presence of pyrrolidine or Bu_4NOAc as base provided 90–99% yields of the coupled products in 2–3 h, but at a much higher temperature of 110 °C. While in the second such example, both the dinuclear $[Pd_2(\mu\text{-}Cl)_2(L'')_2]$ and the mononuclear $[Pd(L'')(PPh_3)Cl]$ (HL″ = 4-methyl-*N*-(ferrocenylidene)aniline) cyclopalladates (1 mol%) along with CuI (2.5 mol%) were examined as the catalyst systems in presence of KOAc as the base for the terminal alkyne homocoupling reactions in dimethylformamide solvent at 40 °C [42]. The reaction showed a broad substrate scope with yields in the range of 42–96%, but the reaction time varied from 2 to 44 h. The reaction time also increases significantly with the decrease of the catalyst loading from 1 mol% to 0.1 mol%. It was also found that the mononuclear complex was more active and efficient than the dinuclear complex. In the present study, change of the catalyst from the mononuclear **2** to the teranuclear **1** keeping the same loading (0.1 mol%) did not affect the reaction time and the yield in any significant way (Table 5, entries 1 and 2). Further, the extents of the increase in the reaction time and the decrease in the yield with the decrease of the catalyst loading were very similar for both complexes (entries 3–8). The reaction time increased 2.5-fold and the yield decreased by about 20% for both **1** and **2** with the decrease of the catalyst loading from 0.1 to 0.001 mol%. Although both **1** and **2** displayed very similar catalytic activities, but the difference in the nuclearities of **1** and **2** suggests that **2** is a better performing catalyst than **1**.

Table 4
Optimization of reaction conditions.[a]

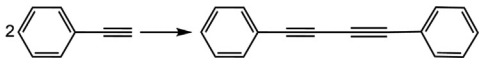

Entry	Base	Solvent	Temp. (°C)	Time (h)	Yield (%)
1	No Base	CH_3CN	60	24	23
2	K_2CO_3 (2 mmol)	CH_3CN	60	16	47
3	Na_2CO_3 (2 mmol)	CH_3CN	60	16	43
4	NaOAc (2 mmol)	CH_3CN	60	18	55
5	$NaHCO_3$ (2 mmol)	CH_3CN	60	24	37
6	NaOH (2 mmol)	CH_3CN	60	24	31
7	DBU (2 mmol)	CH_3CN	60	10	82
8	DABCO (2 mmol)	CH_3CN	60	12	72
9	Et_3N (2 mmol)	CH_3CN	60	12	66
10	PPh_3 (2 mmol)	CH_3CN	60	24	74
11	K_3PO_4 (2 mmol)	CH_3CN	60	04	94
12	K_3PO_4 (1.5 mmol)	CH_3CN	60	04	93
13	K_3PO_4 (1.0 mmol)	CH_3CN	60	10	81
14	K_3PO_4 (0.5 mmol)	CH_3CN	60	12	66
15	K_3PO_4 (1.5 mmol)	$(CH_3)_2NCHO$	60	04	88
16	K_3PO_4 (1.5 mmol)	$C_6H_5CH_3$	60	04	80
17	K_3PO_4 (1.5 mmol)	H_2O	60	12	68
18	K_3PO_4 (1.5 mmol)	CH_3OH	60	04	79
19	K_3PO_4 (1.5 mmol)	$(CH_2)_4O$	60	04	85
20	K_3PO_4 (1.5 mmol)	CH_3CN	25	24	62
21	K_3PO_4 (1.5 mmol)	CH_3CN	40	16	78
22	K_3PO_4 (1.5 mmol)	CH_3CN	80	04	94
23[b]	K_3PO_4 (1.5 mmol)	CH_3CN	60	04	48
24[c]	K_3PO_4 (1.5 mmol)	CH_3CN	60	04	29

[a] Phenylacetylene (1 mmol), **2** (0.1 mol%) in $(CH_3)_2NCHO$ (0.1 ml), CuI (0.5 mol%), base, solvent (1 ml).
[b] Without **2**.
[c] Without CuI.

Table 5
Variation of catalyst and its loading.[a]

Entry	Catalyst	Mol%	Time (h)	Yield (%)
1	**1**	0.1	4 h	96
2	**2**	0.1	4 h	93
3	**1**	0.05	5 h	91
4	**2**	0.05	5 h	91
5	**1**	0.01	6 h	86
6	**2**	0.01	6 h	88
7	**1**	0.001	10 h	78
8	**2**	0.001	10 h	73

[a] Reaction conditions: Phenylacetylene (1 mmol), catalyst in $(CH_3)_2NCHO$ (0.1 ml), CuI (0.5 mol%), K_3PO_4 (1.5 mmol), CH_3CN (1 ml), 60 °C.

4. Conclusions

The capability of *N'*-(9-anthracenylidene)benzothiohydrazide (H_2L) to produce cyclometallated species has been demonstrated.

The cyclopalladated complexes isolated were characterized as the tetranuclear $[Pd_4(L)_4]$ (**1**) and the mononuclear $[Pd(L)(PPh_3)]$ (**2**). X-ray crystal structures of **1** and **2** revealed the pincer-like 5,6-membered fused chelate rings forming thioamidate-S, azomethine-N and 9-anthracenylidene *peri*-C coordination mode of $(L)^{2-}$ and its additional ability to bridge a second metal atom via the thioamidate-S in **1**, leading to a cradle-like $\{Pd_4(\mu\text{-}S)_4\}$ core. The spectroscopic characteristics of **1** and **2** are consistent with the corresponding molecular structures. Both complexes exhibited comparable and decent catalytic activities in the oxidative homo-coupling reaction of phenylacetylene.

Acknowledgements

G. N. Babu thanks the Council of Scientific and Industrial Research, New Delhi for a research fellowship (No. 09/414(1025)/2012-EMR-I). We gratefully acknowledge the financial support provided by the Department of Science and Technology, New Delhi (FIST and PURSE programs) and the University Grants Commission, New Delhi (UPE and CAS programs).

Appendix A. Supplementary material

CCDC 1497686 and 1497687 contain the supplementary crystallographic data for **1**·$CHCl_3$ and **2**·CH_3CN, respectively. These data can be obtained free of charge via http://www.ccdc.cam.ac.uk/conts/retrieving.html, or from the Cambridge Crystallographic Data Centre, 12 Union Road, Cambridge CB2 1EZ, UK; fax: (+44) 1223-336-033; or e-mail: deposit@ccdc.cam.ac.uk.

References

[1] J.P. Kleiman, M. Dubeck, J. Am. Chem. Soc. 85 (1963) 1544–1545.
[2] J. Dupont, M. Pfeffer (Eds.), Palladacycles: Synthesis, Characterization and Applications, Wiley-VCH, Weinheim, 2008.
[3] M. Albrecht, Chem. Rev. 110 (2010) 576–623.
[4] I.P. Beletskaya, A.V. Cheprakov, J. Organomet. Chem. 689 (2004) 4055–4082.
[5] I. Omae, Cyclometalation Reactions, Springer, Tokyo, 2014.
[6] K. Godula, D. Sames, Science 312 (2006) 67–72.
[7] Y. You, W. Nam, Chem. Soc. Rev. 41 (2012) 7061–7084.
[8] N. Cutillas, G.S. Yellol, C. de Haro, C. Vicente, V. Rodríguez, J. Ruiz, Coord. Chem. Rev. 257 (2013) 2784–2797.
[9] X. Jiang, N. Zhu, D. Zhao, Y. Ma, Sci. China Chem. 59 (2016) 40–52.
[10] S. Das, S. Pal, J. Organomet. Chem. 689 (2004) 352–360.
[11] A.R.B. Rao, S. Pal, J. Organomet. Chem. 731 (2013) 67–72.
[12] K. Nagaraju, S. Pal, J. Organomet. Chem. 745–746 (2013) 404–408.
[13] A.R.B. Rao, S. Pal, J. Organomet. Chem. 762 (2014) 58–66.
[14] A.R.B. Rao, S. Pal, J. Organomet. Chem. 797 (2015) 96–100.
[15] R.N. Prabhu, S. Pal, J. Chem. Sci. 127 (2015) 589–596.
[16] G.N. Babu, S. Pal, J. Organomet. Chem. 805 (2016) 19–26.
[17] K. Nagaraju, S. Pal, Inorg. Chim. Acta 413 (2014) 102–108.
[18] D.D. Perrin, W.L.F. Armarego, D.P. Perrin, Purification of Laboratory Chemicals, second ed., Pergamon, Oxford, 1983.
[19] CrysAlisPro Version 1.171.37.34i, Agilent Technologies, Yarnton, Oxfordshire, UK, 2014.
[20] P. van der Sluis, A.L. Spek, Acta Crystallogr. Sect. A 46 (1990) 194–201.
[21] A.L. Spek, Platon, a Multipurpose Crystallographic Tool, Utrecht University, Utrecht, The Netherlands, 2002.
[22] G.M. Sheldrick, Acta Crystallogr. Sect. A 64 (2008) 112–122.
[23] L.J. Farrugia, J. Appl. Crystallogr. 45 (2012) 849–854.
[24] C.F. Macrae, I.J. Bruno, J.A. Chisholm, P.R. Edgington, P. McCabe, E. Pidcock, L. Rodriguez-Monge, R. Taylor, J. van de Streek, P.A. Wood, J. Appl. Crystallogr. 41 (2008) 466–470.
[25] J.M. Antelo, L. Adrio, M.T. Pereira, J.M. Ortigueira, J.J. Fernández, J.M. Vila, Cryst. Growth Des. 10 (2010) 700–708.
[26] P. Pelagatti, A. Venturini, A. Leporati, M. Carcelli, M. Costa, A. Bacchi, G. Pelizzia, C. Pelizzi, J. Chem. Soc. Dalton Trans. (1998) 2715–2721.
[27] P. Paul, S. Bhattacharya, J. Chem. Sci. 126 (2014) 1547–1555.
[28] S. Lentijo, J.A. Miguel, P. Espinet, Dalton Trans. 40 (2011) 7602–7609.
[29] D. Nin-Vien, N.B. Clothup, W.G. Fateley, J.G. Grasselli, The Handbook of Infrared and Raman Characteristic Frequencies of Organic Molecules, Academic Press, London, 1991, pp. 236–238.
[30] H. Du, R.A. Fuh, J. Li, L.A. Corkan, J.S. Lindsey, Photochem. Photobiol. 68 (1998) 141–142.
[31] Z. Bedlovicová, J. Imrich, P. Kristian, I. Danihel, S. Böhm, D. Sabolová, M. Kozurková, H. Paulíková, K.D. Klika, Heterocycles 80 (2010) 1047–1066.
[32] S. Lentijo, J.A. Miguel, P. Espinet, Organometallics 30 (2011) 1059–1066.
[33] P. Siemens, R.C. Livingston, F. Diederich, Angew. Chem. Int. Ed. 39 (2000) 2632–2657.
[34] A.L.K.S. Shun, R.R. Tykwinski, Angew. Chem. Int. Ed. 45 (2006) 1034–1057.
[35] H.A. Stefani, A.S. Guarezemini, R. Cella, Tetrahedron 66 (2010) 7871–7918.
[36] W. Shi, A. Lei, Tetrahedron Lett. 55 (2014) 2763–2772.
[37] W. Shei, Curr. Organocatal 2 (2015) 2–13.
[38] K.S. Sindhu, A.P. Thankachan, P.S. Sajitha, G. Anilkumar, Org. Biomol. Chem. 13 (2015) 6891–6905.
[39] C. Glaser, Ber. Dtsch.Chem. Ges. 2 (1869) 422–424.
[40] C. Glaser, Ann. Chem. Pharm. 154 (1870) 137–171.
[41] D.A. Alonso, C. Nájera, M.A. Pacheco, Adv. Synth. Catal. 345 (2003) 1146–1158.
[42] F. Yang, X. Cui, Y. Li, J. Zhang, G. Rena, Y. Wu, Tetrahedron 63 (2007) 1963–1969.